Journal of NeuroVirology, 12: 73–89, 2006

ISSN: 1355-0284 print / 1538-2443 online
DOI: 10.1080/13550280600654565

Taylor & Francis
Taylor & Francis Group

Simian immunodeficiency virus envelope compartmentalizes in brain regions independent of neuropathology

Maria F Chen,[1] Susan Westmoreland,[2] Elena V Ryzhova,[1] Julio Martín-García,[1] Samantha S Soldan,[1] Andrew Lackner,[3] and Francisco González-Scarano[1]

[1]*Department of Neurology, University of Pennsylvania School of Medicine, Philadelphia, USA*
[2]*Center for Comparative Medicine, Department of Pathology, Massachusetts General Hospital and Harvard Medical School, Boston, Massachusetts, USA*
[3]*Tulane National Primate Research Center, New Orleans, Louisiana, USA*

Simian immunodeficiency virus (SIV) and human immunodeficiency virus (HIV) gp160s obtained from the brain are often genetically distinct from those isolated from other organs, suggesting the presence of brain-specific selective pressures or founder effects that result in the compartmentalization of viral quasispecies. Whereas HIV has also been found to compartmentalize within different regions of the brain, the extent of brain-regional compartmentalization of SIV in rhesus macaques has not been characterized. Furthermore, much is still unknown about whether phenotypic differences exist in envelopes from different brain regions. To address these questions, *env* DNA sequences were amplified from four SIVmac239-infected macaques and subjected to phylogenetic and phenetic analysis. The authors demonstrated that sequences from different areas of the brain form distinct clades, and that the long-term progressing macaques demonstrated a greater degree of regional compartmentalization compared to the rapidly progressing macaques. In addition, regional compartmentalization occurred regardless of the presence of giant-cell encephalitis. Nucleotide substitution rates at synonymous and nonsynonymous sites (ds:dn rates) indicated that positive selection varied among envelopes from different brain regions. In one macaque, envelopes from some but not all brain regions acquired changes in a conserved CD4-binding motif GGGDPE at amino acids 382 to 387. Furthermore, gp160s with the mutation G383E were able to mediate cell-to-cell fusion in a CD4-independent manner and were more susceptible to fusion inhibition by pooled plasma from infected macaques. Reversion of this mutation by site-directed mutagenesis resulted in reduction of CD4-independence and resistance to fusion inhibition in cell fusion assays. These studies demonstrate that SIV evolution within the brain results in a heterogeneous viral population with different phenotypes among different regions. *Journal of NeuroVirology* (2006) **12,** 73–89.

Keywords: CD4-independence; CNS compartmentalization; gp160; SIV

Introduction

Human immunodeficiency virus (HIV) and simian immunodeficiency virus (SIV) infections are characterized by the generation of numerous viral variants due to the massive turnover of viral particles within the host (Coffin, 1995; Perelson *et al*, 1996). With progression of infection there may be development of specific signature sequences, presumably because of selective constraints imposed by the immune system, or through preferential tropism for target cells, or due to other selection pressures imposed such as

Address correspondence to Francisco González-Scarano, Department of Neurology, University of Pennsylvania, 3 West Gates, 3400 Spruce Street, Philadelphia, PA 19104-4283, USA. E-mail: scarano@mail.med.upenn.edu

The present address of Julio Martín-García is Department of Microbiology and Immunology, Drexel University College of Medicine, Philadelphia, Pennsylvania, USA

This work was supported by PHS grants MH-067734 and NS-27405. The authors thank Pyone Aye (Tulane National Primate Research Center for) for the gift of reagents and Bridget Puffer, George Leslie, George Lin, Robert Doms, and James Hoxie (University of Pennsylvania) for helpful discussions.

Received 27 October 2005; revised 16 January 2006; accepted 7 February 2006.

drug-resistance (Crandall *et al*, 1999; Kimata *et al*, 1999; Kodama *et al*, 1993; Wolinsky *et al*, 1996). In the setting of a chronic infection, viral variants can form distinct quasispecies limited to a particular tissue compartment (Campbell and Hirsch, 1994; Fulcher *et al*, 2004; Poss *et al*, 1998; Wang *et al*, 2001; Zhang *et al*, 2002). The nature of HIV/SIV evolution in the brain is of specific interest because, unlike most non-neuronal tissues that support infection, the brain is a somewhat immunologically privileged site and the level of viral replication in the brain is low compared to compartments where there are more CD4+ T cells (Gendelman *et al*, 1994; Glass *et al*, 1995; Price *et al*, 1988; Vazeux *et al*, 1992). Hence, the diversification, compartmentalization, and adaptation of virus in the brain may be independent from that occurring in lymphoid tissues that are exposed to immune pressures and where virus replication is more robust.

Understanding the evolution and adaptation of HIV/SIV in the brain will help determine the viral factors that contribute to retrovirus-associated neurological disease. Before the advent of highly active antiretroviral therapy (HAART), HIV-associated dementia (HAD) affected 15% of those infected whereas another 15% experienced a less severe form of cognitive impairment called minor cognitive motor disorder (MCMD) (McArthur *et al*, 1999). Although the incidence of HAD has dropped significantly since the widespread use of HAART, the prevalence of less severe cognitive disorders is still high (Sacktor *et al*, 2001a, 2002). Furthermore, some antiretroviral drugs do not penetrate the central nervous system (CNS); even with viral suppression, the brain harbors latently infected cells that may be a potential source of virus after the withdrawal of therapy (Clements *et al*, 2002; Ryzhova *et al*, 2002b; Sacktor *et al*, 2001b). This problematic feature of a latent infection in the midst of nonsterilizing therapy reinforces the need to understand viral features that are responsible for pathology in the brain.

Several groups have shown that viral envelopes with genotypes that support viral replication in the brain are linked to the development of the neuropathological hallmarks of HIV/SIV encephalitis or HAD (Anderson *et al*, 1993; Babas *et al*, 2003; Peters *et al*, 2004; Power *et al*, 1994; Zink *et al*, 1997). Envelope gp160s that are macrophage-tropic as determined either by direct analysis or indirectly by sequence signatures have been isolated from the brains of individuals and macaques with and without giant-cell encephalitis. This suggests that infection of brain macrophages and microglia is necessary but not sufficient for the development of giant-cell encephalitis (Gorry *et al*, 2001; Kodama *et al*, 1993; Korber *et al*, 1994; Mankowski *et al*, 1997). One potential envelope feature that promotes infection in the brain may be the ability to mediate fusion on the target cells that express low levels of the receptor CD4. This could be an adaptive feature, because microglia and brain macrophages express lower levels of CD4 on their surface in comparison with CD4+ T cells (Wang *et al*, 2002). Envelopes with reduced dependence on CD4 may evolve in the CNS where there is diminished humoral immunity, because these envelopes tend to have exposed coreceptor binding sites and are therefore easier to neutralize (Bhattacharya *et al*, 2003; Kolchinsky *et al*, 2001; Martin *et al*, 2001). In the absence of this humoral immunity-mediated selective pressure in the brain and in rapidly progressing macaques that fail to mount an effective antibody response, mutations resulting in reduced CD4 dependence may be more likely to be fixed and hence predominate (Dehghani *et al*, 2003; Ryzhova *et al*, 2002a).

SIV-infected rhesus macaques have a disease course with neuropathology similar to humans infected with HIV (Fox *et al*, 1997; Lackner *et al*, 1991; Prospero-Garcia *et al*, 1996). Whereas regional compartmentalization of HIV gp160 in human brains has been previously documented, no studies to date have characterized the degree of SIV env compartmentalization with regard to neuropathology or disease progression in the CNS of macaques (Liu *et al*, 2000; Salemi *et al*, 2005; Shapshak *et al*, 1999; Smit *et al*, 2001). Characterization of virus evolution in macaques is important because macaque studies can differ from human studies in the use of a defined molecularly cloned virus inoculum. Hence, the compartmentalization seen in human studies, which may partly result from the selective migration to specific anatomical sites by different variants acquired at transmission, may be different in macaques intravenously inoculated with a clonal virus. Furthermore, knowledge of the precise length of infection in macaque studies allows us to correlate the extent of compartmentalization with disease progression.

To characterize SIV env evolution in the macaque CNS, we analyzed gp160s cloned from genomic DNA, which provides a "history" of the infection of various brain regions. Using archived tissue from macaques infected with a molecularly cloned SIVmac239 with different disease progressions (two rapid versus two long-term), we addressed the question of whether chronicity of infection is required for gp160 compartmentalization in the brain. Within each type of disease progression, we also compared whether gp160 compartmentalizes in the brain differently with respect to presence of giant-cell encephalitis. To determine whether certain viral genotypes would be favored in the brain, we calculated rates of synonymous and nonsynonymous change for an indication of positive selection. Furthermore, we looked for amino acid mutations in key functional regions of gp160 that result in advantageous phenotypes. These studies provide additional insight into SIV variation in the CNS and genotypes and phenotypes that may arise in brain and potentially contribute to pathology.

Results

Phylogenetic tree construction of envelopes cloned from CNS and non-CNS tissue of SIVmac239-infected macaques

Four SIVmac239-inoculated macaques were selected on the basis of their systemic progression and their neuropathological findings (Table 1). The entire *env* sequence was cloned from the genomic DNA of several CNS regions and from available extra-CNS tissues (spleen for macaque 362, mesenteric lymph node for macaques 190 and 264, inguinal lymph node for macaque 247, lung for macaque 190, colon for macaques 247, 264, 362). Four to eight clones from each tissue region were directly sequenced, aligned, and subjected to phylogenetic analysis using both distance-based (neighbor-joining) and character-based (maximum parsimony and maximum likelihood) methods. Same-tree topologies and similar bootstrap values were derived for all three methods for each macaque, and the maximum likelihood trees are shown as representative trees in Figure 1. Because all of the macaques were inoculated with the SIVmac239 clone, the trees were rooted to this sequence.

Trees of the long-term progressing macaques with or without giant-cell encephalitis (macaque 247, Figure 1A; macaque 190, Figure 1B, respectively) demonstrated robust regional compartmentalization of gp160 as seen in the formation of tissue-based monophyletic clades with strong bootstrap support (values >50 at nodes). Exceptions were the gp160s from the spinal cord of macaque 247 (which formed two distinct clades), the periventricular brain tissue of the same animal, which formed a distinct clade that was not supported by a high bootstrap value, and clones from the lung of macaque 190, which were spread throughout the macaque 190 tree.

Furthermore, gp160s from the CNS compartments of these two long-term progressing macaques shared their most recent common ancestors with clades from different non-CNS tissues. This finding supports the hypothesis that there are multiple independent entry events into the CNS (Figure 1A, B). For example, the clade formed by the cerebrum of macaque 247 shared a most recent common ancestor with the superclade formed by multiple sister clades from the cerebellum, colon, spinal cord and inguinal lymph node (Figure 1A). In comparison, the clade from its cerebellum shared a most recent common ancestor with the envelopes amplified from the colon, indicating an entry event into the cerebellum that is distinct from that in the cerebrum. The phylogenetic tree of macaque 190 also supported multiple neuroinvasion events (Figure 1B); the brain clades from this macaque shared their most recent common ancestors with non-neuronal clades rather than forming one superclade consisting of brain envelopes only.

In comparison, although the tree of the rapidly progressing macaque with giant-cell encephalitis showed compartmentalization (macaque 264, Figure 1C), as exemplified by the clades formed by cerebrum, colon, and periventricular brain tissue, the monophyletic clusters were not supported by significant bootstrap values with the exception of the cerebral clade. In the rapidly progressing macaque *without* giant-cell encephalitis (362, Figure 1D), the extent of gp160 compartmentalization in the CNS was even less defined. Sequences from the periventricular area and the brainstem were dispersed throughout the tree indicating more gene flow in the brain of this macaque potentially due to increased trafficking of virus into the brain. The pattern and bootstrap support of compartmentalization shown in the phylogenetic trees indicate that the duration of the infection, rather than the manifestation of giant-cell encephalitis contributed to the emergence of regionally distinct viral quasispecies in the CNS.

Phylogenetic and phenetic evaluation of tissue compartmentalization

Because the monophyletic clades from the rapidly progressing macaques were not supported by the bootstrap analysis, the inference of tissue compartmentalization based on the topology of the phylogenetic trees could be inaccurate. To clarify this, both cladistic (phylogenetic) and distance-based (phenetic) methods were used; these test for the presence of compartmentalization without the need for an accurate evolutionary history and also allow for a quantification of the degree of compartmentalization. The

Table 1 Summary of clinical and necropsy data

Animal (necropsy) no.	*Survival (days, post inoculation)*	*Disease progression*[a]	*SAIDS*[b]	*Neuropathological*[c] *findings*
247	320	Long-term	+	Giant cell encephalitis
190	416	Long-term	+	Mild encephalitis without giant cells
264	176	Rapid	+	Giant cell encephalitis
362	93	Rapid	+	Mild encephalitis without giant cells

[a]Long-term progression defined as survival >200 days, rapid progression <200 days, according to Westmoreland (1998).
[b]SAIDS = simian acquired immunodeficiency syndrome.
[c]For macaques 190 and 362, characterized as having mild encephalitis without giant cells, the extent of the inflammatory changes were mild as determined by pathologists at the New England Regional Primate Research Center.

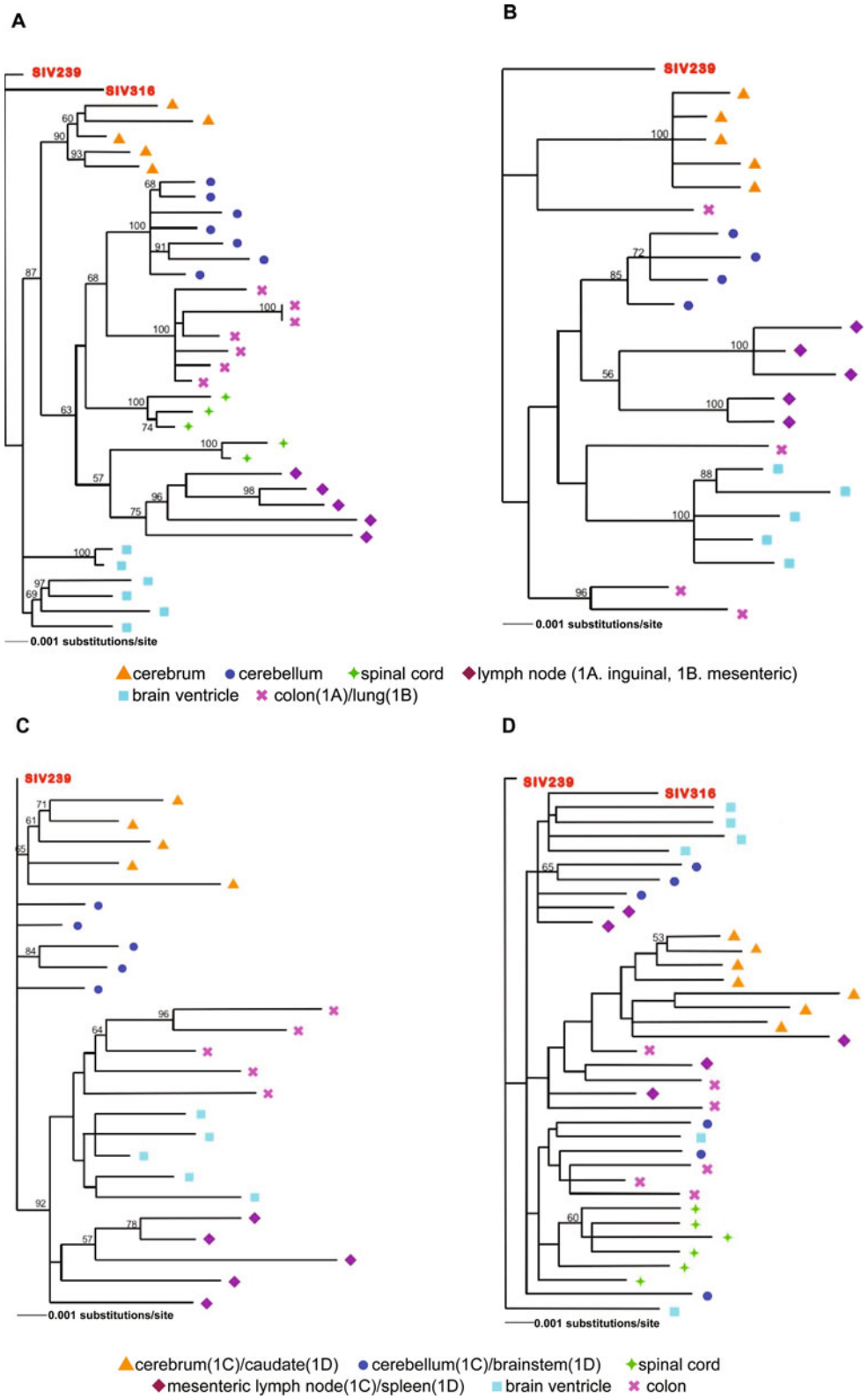

Figure 1 Compartmentalization of gp160s isolated from various tissues of SIVmac239-infected rhesus macaques. *Env* genes were cloned from the genomic DNA of long-term progressing macaques 247 (**A**) and 190 (**B**) and rapidly progressing macaques 264 (**C**) and 362 (**D**) from the following tissues: ▲ (cerebrum for macaques 247, 190, and 264, caudate for macaque 362), ● (cerebellum for macaques 247, 190, and 264, brainstem for macaque 362), ✦ (spinal cord), ■ (brain ventricle), ✖ (colon for macaques 247, 264, 362, lung for macaque 190), ♦ (lymph node, mesenteric for macaques 190, 264, inguinal for macaque 247/spleen for macaque 362). The phylogenetic trees were derived from maximum likelihood analysis; those determined by parsimony and distance analysis were similar. Bootstrap values were performed on 100 pseudoreplicate data sets and those >50 are indicated at the nodes. Nodes where no value is indicated were not supported at this level.

cladistic method is the Slatkin-Maddison test, modified to account for phylogenetic uncertainty (Poss *et al*, 1998; Slatkin and Maddison, 1990). Gp160 sequences from all four macaques demonstrated statistically significant tissue compartmentalization by the Slatkin-Maddison test, as the number of migration steps from complete compartmental structure (no migration) was less for the bootstrap trees in comparison with the random trees. This significance in difference is indicated by ratios of bootstrap steps to random tree steps of less than 1 (ratio of 0.30 ± 0.03 for macaque 247, 0.35 ± 0.04 for macaque 190, 0.38 ± 0.08 for macaque 264, and 0.68 ± 0.07 for macaque 362). Although the sequences from the four macaques demonstrated compartmentalization, in the rapidly progressing macaque without giant-cell encephalitis, macaque 362, this evidence was less robust than in the other three macaques ($P < .001$, t test).

Mantel's test was performed on envelope sequences from all four macaques to determine whether sequences from the same tissue or brain region demonstrate compartmental structure based on genetic identity (Mantel, 1967). Evidence of compartmentalization using Mantel's test is signified with a sample Pearson's correlation coefficient that is greater than the correlation coefficients of randomizations of the same data set. A compartment structure was supported by Mantel's test for all four macaques ($P < .001$; Table 2). Furthermore, the larger Pearson's correlation coefficient (r) of the two long-term progressing macaques, 247 and 190 ($r = .573$ and .709, respectively), compared with the two rapidly progressing macaques, 264 and 362 ($r = .276$, .182, respectively), also supports the conclusion of robust compartment structure developing with a longer duration of infection. There was no association between giant-cell encephalitis and compartmentalization of gp160 in the phenetic analysis.

Synonymous and nonsynonymous nucleotide substitution rates

Tissue-specific compartmentalization can result from selection of a genotype by the specific environment of that compartment, or by a "founder" effect due to the isolated replication of a few genotypes. One way to begin to distinguish between these two possibilities is to determine the relative rates of nucleotide substitution at synonymous and nonsynonymous sites (ds and dn) because a greater dn compared to ds indicates the presence of positive selection (Sharp, 1997). Using the SIVmac239 sequence as the origin, the nucleotide substitutions (excluding insertions and deletions) in each gp160 sequence were counted, and the average ds and dn were then determined for each tissue or region (Figure 2A, B).

With the exception of the spinal cord of animal 247, the cerebrum and cerebellum of macaque 190, and the macaque 264 periventricular area, the dn rates were lower than the ds rates for all compartments,

Table 2 Phenetic evaluation by Mantel's test of env compartmentalization

Animal (necropsy) no.	*Pearson's correlation coefficient*	*Pearson's correlation coefficient of null distribution*[a]	*P value*
247	.573	$.002 \pm .045$	<.001
190	.709	$-.0061 \pm .060$	<.001
264	.276	$.002 \pm .025$	<.001
362	.182	$-.003 \pm .021$	<.001

[a]Average correlation coefficient ±1 standard deviation of 1000 permutations of the compartment matrix.

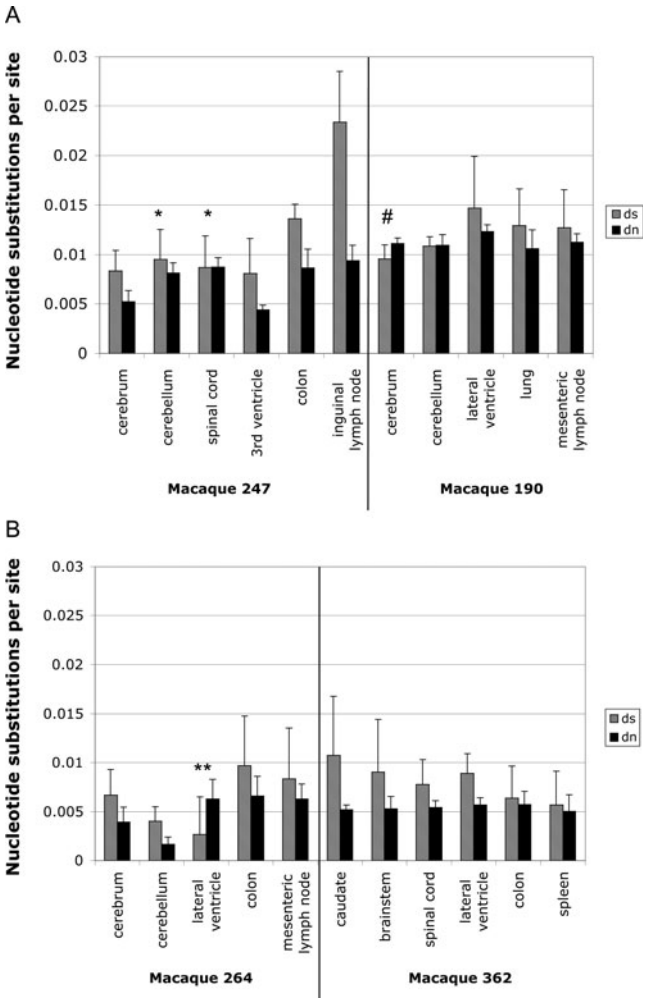

Figure 2 Rate of substitution at synonymous and nonsynonymous sites. Gp160 nucleotide sequences isolated from different tissues of long-term progressing macaques (**A**) or rapidly progressing macaques (**B**) were compared to the sequence of the starting molecular clone of SIVmac239 virus. The numbers of nucleotide changes leading to synonymous and nonsynonymous mutations were tallied using MEGA. *dn of macaque 247 cerebellum and spinal cord less than dn of macaque 247 cerebrum and 3rd ventricle, $P < .01$, Mann-Whitney U. **dn of macaque 264 lateral ventricle less than macaque 264 cerebellum, $P < .05$, Mann-Whitney U. #ds:dn <1, hence significant for positive selection, $P < .05$, t test.

suggesting that positive selection was not the predominant force driving the evolution of these envelopes. Envelopes from the macaque 247 spinal cord, the macaque 190 cerebrum and cerebellum, and the macaque 264 periventricular region had dn rates greater than ds rates. However, this was only statistically significant for envelopes of macaque 190 cerebrum ($P < .05$, *t* test). Interestingly, all five envelopes cloned from the macaque 190 cerebrum contained a 6–amino acid deletion in V4, a region that is an important antibody recognition site (415-NTANQK-420; Figure 3A) (Kinsey *et al*, 1996). This deletion was not present in any of the other regions, and only in 1/9 extra-CNS envelopes isolated. However, all of the other envelopes from this macaque contained a different change in this same V4 region, all of them with a potential new glycosylation site. In addition, macaque 190 cerebrum envelopes were the only brain envelopes from this macaque to retain a potential *N*-glycosylation site at amino acid 370, which was lost in all other brain envelopes. The pattern of sequence changes in the V4 region in addition to a ds and dn rates significant for positive selection suggests that escape from immune response may have shaped the evolution of envelopes isolated from the brain of this macaque.

Although very few of the ds and dn rates signify the overt presence of positive selection, differences in relative rates of ds and dn were noted in different brain regions of the same macaque, suggesting that some envelopes acquired different mutations that might correlate to some functional difference. For example, although all four brain regions of long-term progressing encephalitic macaque 247 had similar ds rates (0.0081 to 0.0095), the dn rates for the spinal cord and cerebellum (respectively, 0.0087 ± 0.0009 and 0.0082 ± 0.0010) were greater than those of the cerebrum and periventricular brain region (Figure 2; 0.0052 ± 0.0011 and 0.0044 ± 0.0004; $P < .01$ for all comparisons by Mann-Whitney's *U* test). Likewise, differences with dn were also found in different brain compartments of the rapidly progressing, encephalitic macaque 264 ($dn = 0.0063 \pm 0.0020$ for periventricle, 0.0039 ± 0.0015 for cerebrum, significantly greater than $dn = 0.0017 \pm 0.0008$ for cerebellum; $P < .05$ Mann-Whitney's *U* test).

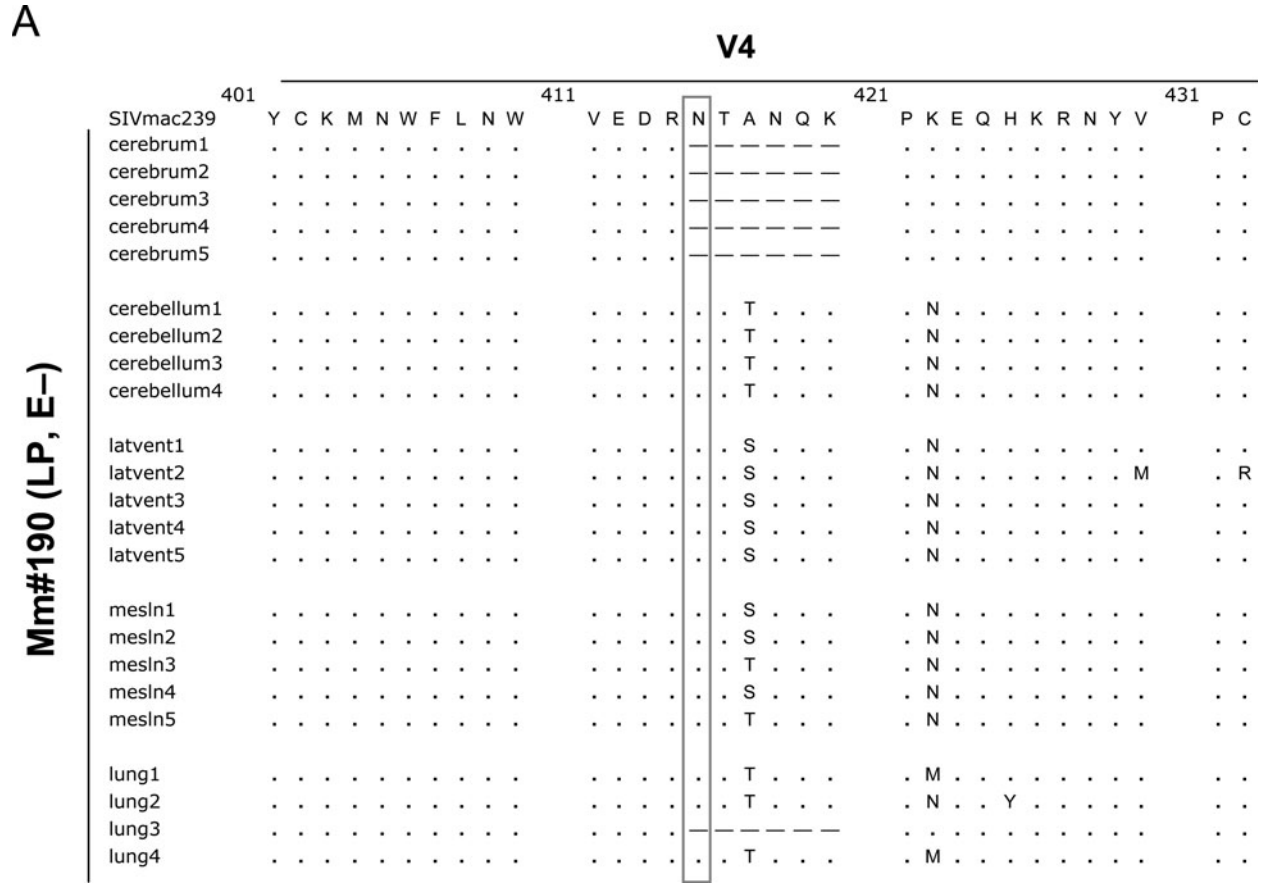

Figure 3 Amino acid changes in key functional regions compared to SIVmac239 gp160 sequence. Regional differences were observed in (**A**) V4 loop and (**B**) V1/V2 loops and (**C**) V3 and CD4-binding domains. Dots indicate no change from the SIVmac239 sequence; dash indicates deletion of the amino acid codon, a letter indicates the amino acid change has occurred; X indicate a nucleotide deletion resulting in a frameshift; A box indicates gain or loss of a potential *N*-glycosylation site. LP = long-term progressor; RP = rapid progressor; E+/E− = encephalitic/nonencephalitic; latvent = lateral ventricle; mesln = mesenteric lymph node. *(Continued)*

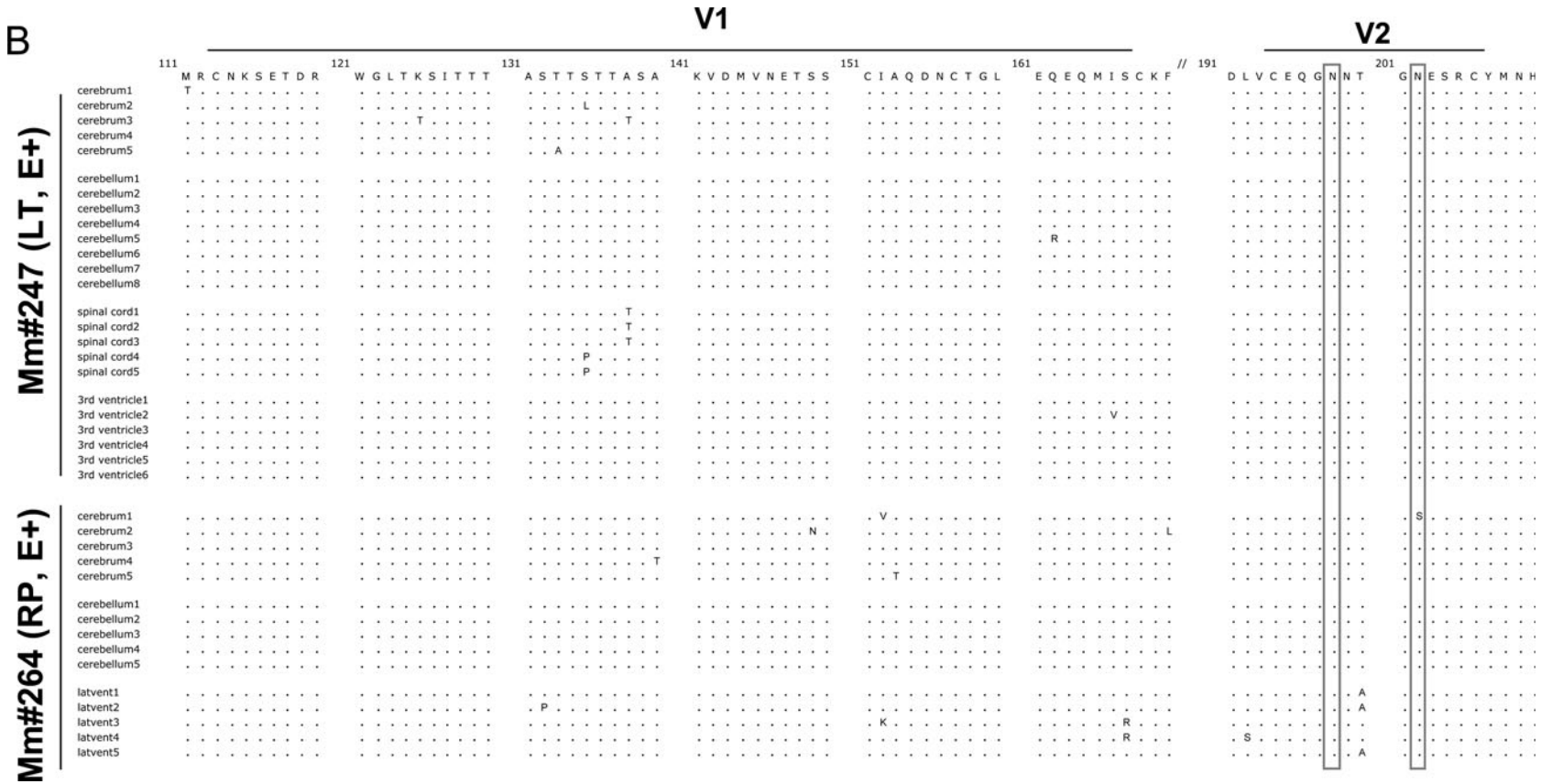

Figure 3 (Continued)

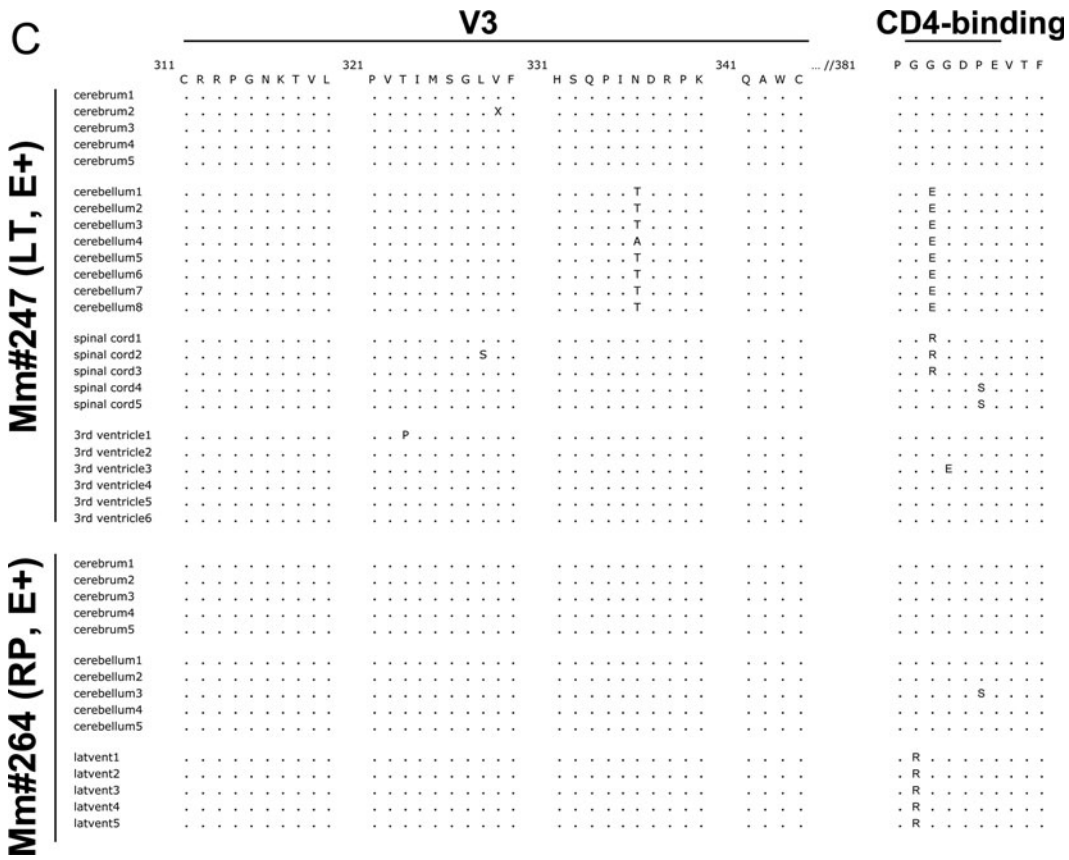

Figure 3 (Continued)

Genotypic analysis

To determine whether envelopes with greater dn rates from the two encephalitic macaques may have acquired adaptive mutations, we examined the envelope gp120 sequences for conserved mutations from the initial SIVmac239 sequence. Surprisingly, there were few amino acid changes in V1/V2 (Figure 3B and data not shown), a region that has been previously demonstrated to acquire the most mutations during the course of SIV infection (Hirsch *et al*, 1998; Overbaugh *et al*, 1991). In macaque 247, although CNS envelopes acquired changes in V1/V2 at K125, T133, S135, A138, Q162, I166, M172, and A190, these mutations were not conserved in all of the envelopes from one region nor did they occur in a majority of the envelopes from various regions. Mutations in the V3 loop were found at N336 in 7/7 cerebellum envelopes from macaque 247 (Figure 3C). Mutations also occurred at amino acids 323 and 328 for spinal cord envelopes, although none of these mutations resulting in gain or loss of a potential *N*-glycosylation site nor were they present in a majority of the envelopes. In macaque 264 there were changes in V1/V2 that affected potential *N*-glycosylation sites (Figure 3B and data not shown). Mutation T186I resulted in the loss of a potential site at 184 in a cerebellum envelope. Likewise a cerebrum envelope lost a potential glycosylation site at position 202, and 3/5 envelopes from the periventricle brain region lost a glycosylation site at amino acid 198 due to T200A. No amino acid mutations were found in the V3 loop sequences in the brain envelopes of macaque 264 (Figure 3C). Overall, the lack of shared mutations in the V1/V2 and V3 loops of the two encephalitic macaques suggests that the mutations acquired in these regions were not likely to have been adaptive mutations.

Despite no conservation of mutations in the V1/V2 and V3 loops of macaques 247 and 264, a notable pattern of mutations was observed in the GGGDPE motif at positions 382 to 388, which forms a part of the CD4 binding domain (Figure 3C). This motif has been previously predicted to line a cavity of gp120 involved with CD4 binding and specifically, the aspartic acid D385 forms key contacts with amino acid residues of CD4 in previous crystallography studies of HIV and SIV gp120 (Chen *et al*, 2005; Kwong *et al*, 1998). Envelopes from three of the four macaques in this study acquired a mutation in this motif. Of interest, in two of these macaques, mutations in this region were acquired by envelopes from brain regions with the higher dn rates, signifying a greater degree of positive selection. In macaque 247 the cerebellar envelopes acquired a G → E change at amino acid 383. A 383G → R change was also present in 3/5 spinal cord envelopes, the other two acquired a P → S mutation at 386. The cerebrum envelopes from this

macaque did not have mutations in this region, and only 1/6 periventricle envelopes acquired a mutation at 384 (G → E). In contrast to macaque 247, which had giant-cell encephalitis, macaque 190 without giant-cell encephalitis did not have any changes in this CD4-binding region.

The other encephalitic macaque, the rapid-progressing macaque 264 also had changes in the CD4-binding region. The brain compartment with the highest dn rate in this macaque, the periventricle, had a G → R mutation at amino acid 382 in 5/5 envelopes. A mutation in this motif was not present in any of the cerebrum envelopes and only 1/5 cerebellum envelopes had a mutation (P → S) at amino acid 386.

The rapidly progressing nonencephalitic macaque 362 also acquired changes in this CD4-binding region. The predominant mutation in this macaque was a change D385 → N occurring in 32 out of 35 brain envelopes sampled across four brain regions (data not shown). Of these 32, 12 had an accompanying mutation at amino acid 383 also present in all four brain compartments sampled. The same D385N mutations in this CD4-binding region were previously identified in rapidly progressing macaques and shown to result in a decreased binding affinity for CD4 (Ryzhova *et al*, 2002a).

CD4-independent and neutralization-sensitive cell-to-cell fusion mediated by envelopes from cerebellum of long-term progressing encephalitic macaque 247

The occurrence of convergent evolution in this CD4-binding motif in addition to higher dn rates suggestive of positive selection lead us to hypothesize that the brain envelopes from the spinal cord and cerebellum of the encephalitic macaque 247 may have adaptive features such as the ability to function independently of CD4. The macaque 247 cerebellum envelopes were chosen for further study because all 7/7 envelopes isolated had acquired a mutation at amino acid 383. Envelopes from the macaque 247 cerebellum were examined in cell-cell fusion assays, a commonly used assay for probing receptor usage by HIV and SIV envelopes (Edinger, 1999; Puffer *et al*, 2004). Four of seven cerebellar envelopes were functional in a cell-to-cell fusion assay using rhesus CCR5 and rhesus CD4 (data not shown). These functional envelopes were then tested for their ability to mediate fusion in the absence of CD4 with the two envelopes representing the two extremes of the range of CD4-independence, shown in Figure 4A. Cerebellar envelopes were able to mediate CD4-independent cell fusion similar or better to a control envelope SIV316 that was previously shown to be able to mediate CD4-independent cell-cell fusion (Puffer *et al*, 2004).

Envelopes that are able to mediate CD4-independent cell fusion often demonstrate enhanced neutralization sensitivity to serum of SIV/HIV-infected subjects, suggestive of an envelope conformation that has an exposed and intact coreceptor binding site (Kolchinsky *et al*, 2001; Lin *et al*, 2003; Puffer *et al*, 2002). To determine whether these CD4-independent envelopes were more neutralization sensitive, cell-to-cell fusion assays were performed in the presence of increasing concentrations of pooled plasma from SIVmac239-infected macaques (Figure 4B). CD4-independent envelopes from the cerebellum of macaque 247 were neutralized with low concentrations of plasma (plasma dilutions of 1:5000 and 1:500), unlike the parental envelope SIVmac239 and a brain (cerebrum) envelope from the same macaque 247 that does not have the G383E mutation. The latter were minimally neutralized at a dilution of 1:50 of the pooled plasma.

Mutagenesis of E383 back to parental glycine (G) of SIVmac239 and testing of CD4-independence and neutralization sensitivity of reversion envelopes

To determine whether the G383E mutation found in the macaque 247 cerebellar envelopes contributed to the CD4-independent phenotype, this position was mutated back to the glycine present in parental SIVmac239 sequence using a cerebellum envelope that acquired the fewest number of amino acid changes (cerebellum 3) and cell-to-cell fusion assays were performed (Figure 5A). CD4-independent fusion of the wild-type cerebellum 3 envelope was more than 400% that of the reversion envelope (247cerebellum3-E383G), suggesting that the E383 contributes significantly to the ability of the 247cerebellum3 envelope to mediate fusion in the absence of CD4. To determine whether the G383E mutation was also responsible for the neutralization-sensitive phenotype, cell-to-cell fusion assays were again performed in the presence of neutralizing plasma (Figure 5B). The reversion envelope 247cerebellum3-E383G demonstrated more fusion in the presence of neutralizing plasma compared to the wild-type 247cerebellum3 envelope, indicating that the reversion envelope was more resistant to neutralization in comparison with the original cerebellar envelope.

Discussion

The identification of brain-specific HIV and SIV envelopes has led many investigators to hypothesize that adaptation of envelopes for the CNS environment may result in viruses with an enhanced ability to replicate in the CNS and/or mediate neuropathology (Anderson *et al*, 1993; Kodama *et al*, 1993; Peters *et al*, 2004; Power *et al*, 1994; Zink *et al*, 1997). However, the study of evolution of virus in the CNS may be further complicated by isolated microenvironments within the CNS with various genotypes and phenotypic profiles (Liu *et al*, 2000; Shapshak *et al*, 1999; Smit *et al*, 2001). Furthermore, the existence of discrete subpopulations argues that the evolution of virus in the CNS may not occur by a selective

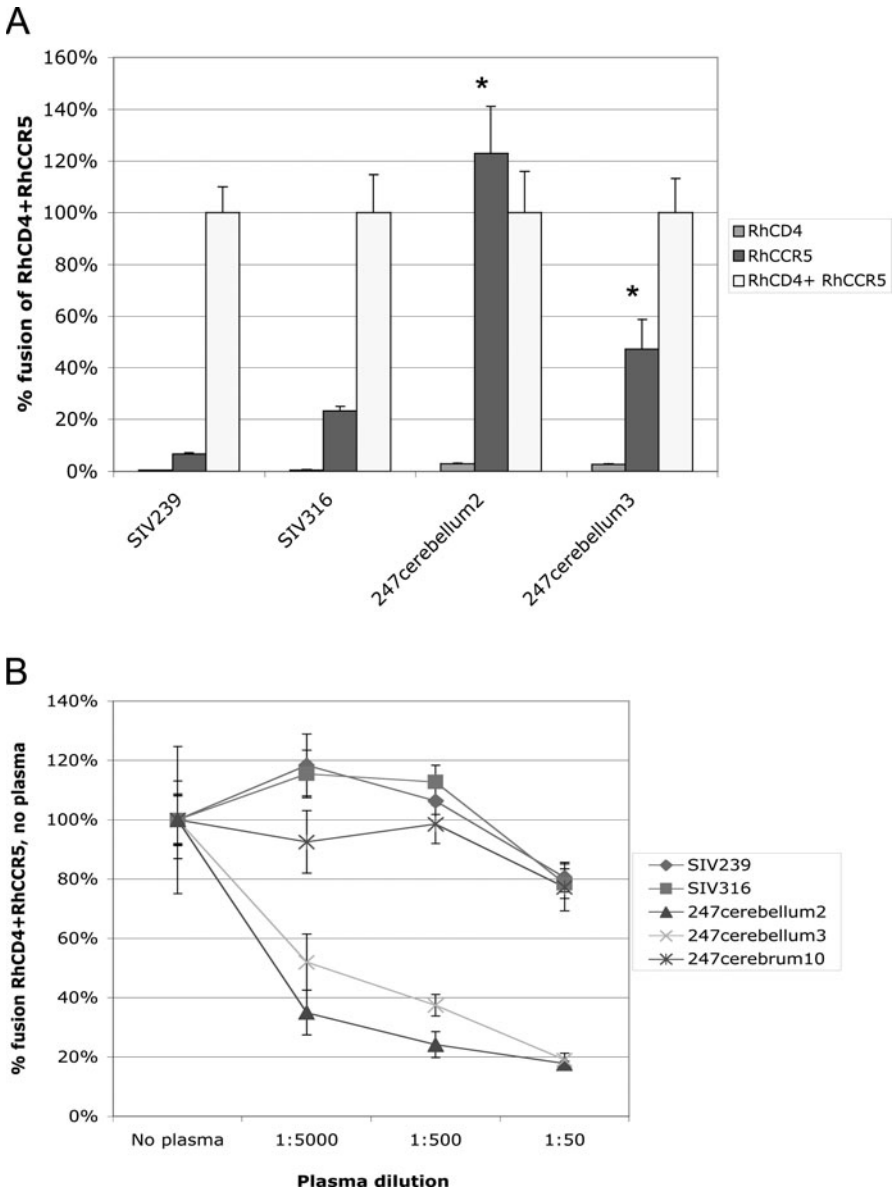

Figure 4 Cell-cell fusion assays of brain gp160s from long-term progressing encephalitic macaque 247. QT6 cells transiently expressing gp160s with mutation G383E (**A**) were overlayed onto target cells expressing either rhesus CCR5 alone or rhesus CCR5 and rhesus CD4, to determine whether envelopes are able to mediate CD4-independent cell-cell fusion. SIVmac239 and SIV316 gp160s were included as CD4-dependent and CD4-independent controls respectively. *RhCCRS fusion levels of 247cerebellum2 gp160 and 247cerebellum3 gp160 greater than RhCCRS fusion levels of SIV316, the positive control gp160 for a CD4-independent envelope, $P < .01$. In (**B**), the experiments were performed with an additional incubation step. The gp160-expressing cells were exposed for 1 h, at 4°C with the indicated dilutions of heat-inactivated pooled plasma from SIVmac239-infected macaques to test for neutralization sensitivity. 247cerebrum10 gp160 was included as an envelope from the brain of the same encephalitic macaque that did not have the G383E mutation. Values are denoted as percentage of fusion activity in cells expressing rhesus CD4 and rhesus CCR5 when no plasma was present.

process, because the effective population size of a single site may be at a low level; circumstances where random genetic drift is favored over adaptive processes (Brown, 1997; Shriner *et al*, 2004).

This study was undertaken to address issues of regional evolution in the CNS of SIV-infected macaques, because macaques are common models for neuro-AIDS (acquired immunodeficiency syndrome), and because to date no studies have reported discrete neuroanatomical localization in macaques. The genetic variation seen in the human CNS may not be present in situations such as macaque infections where the inoculum is a molecular clone. Should the compartmentalized effect seen in human infection be a consequence of selective migration to distinct sites by certain variants, compartmentalization of virus in macaques could be different, because the inoculated virus is molecularly homogeneous. Similar to previous studies of HIV gp160 evolutionary diversity, we utilized viral DNA, thus providing a history of the

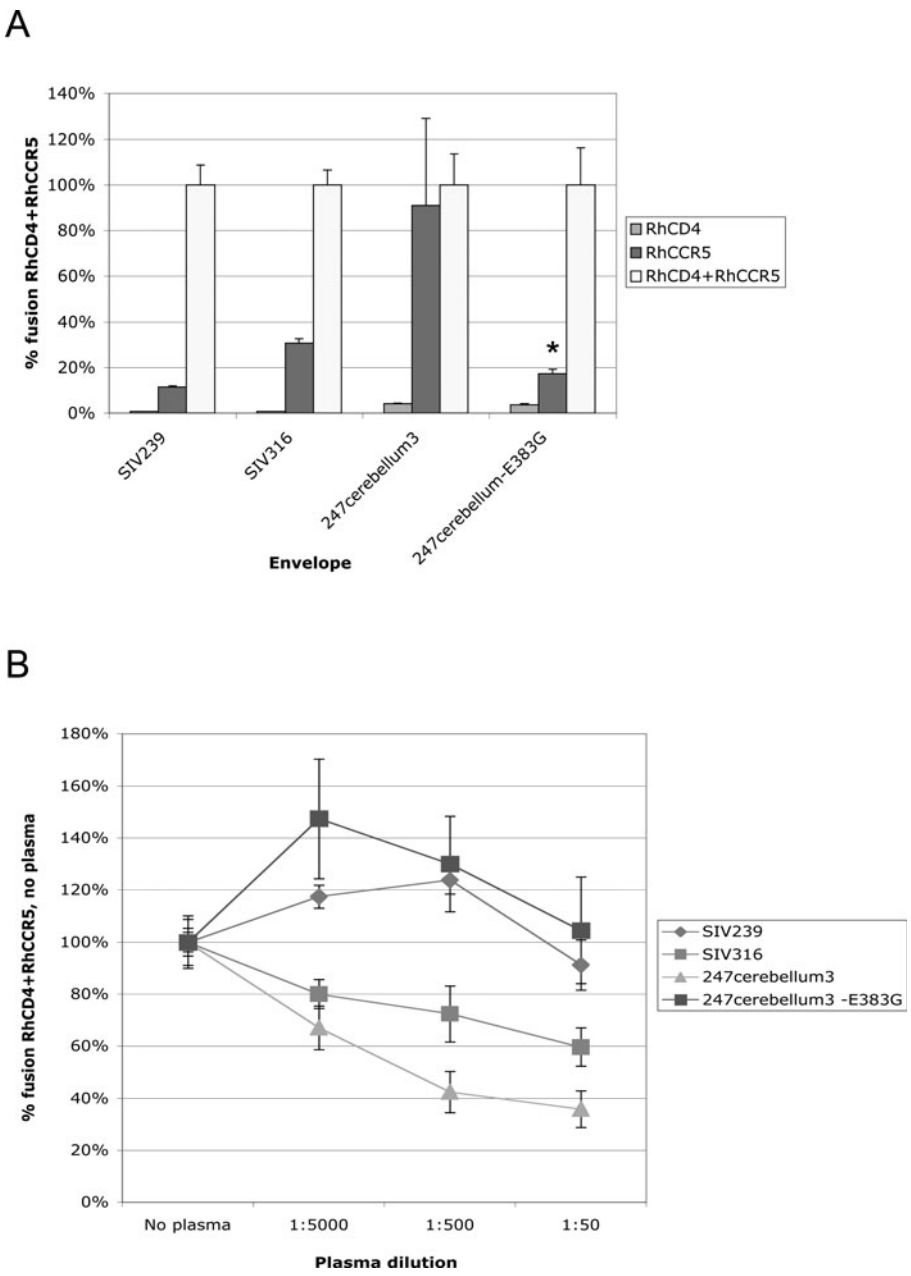

Figure 5 Cell-cell fusion assays of SIVgp160 with glutamic acid (E) 383 reverted back to glycine (G). Gp160s from the brain of macaque 247 containing a G383E change were reverted back to the G383 of SIVmac239 and tested in cell-cell fusion assays. (**A**) *RhCCRS fusion levels for 247cerebellum3-E383G gp160 is less than SIV316, the positive control for CD4-independent fusion, $P < .01$. Data for the original 247cerebellum3 and the reversion envelope 247cerebellum3-E383G are shown as representative experiments for multiple envelopes tested. (**B**) These reversion envelopes were also tested for their sensitivity to neutralization by pooled plasma as described in Figure 4B.

infection (Korber *et al*, 1994; Ohagen *et al*, 2003; Salemi *et al*, 2005; Shapshak *et al*, 1999). As such, the genotypes isolated are those that were present at some point in the history of the infection and may not necessarily include the genotype(s) of the actively replicating pool.

The variation and compartmentalization of SIV envelopes was examined in four rhesus macaques that were infected with the clonal SIVmac239. Consistent with previous reports, there was evidence of compartmentalization of SIV envelope sequences in the CNS of all macaques (Shapshak *et al*, 1999; Smit *et al*, 2001, 2004). The degree of compartmentalization was more robust in the two long-term progressing macaques than in the two rapidly progressing macaques. This relationship suggests that the compartmentalization results from the isolated replication of virus within a particular region, rather than

from the preferential movement of a certain variants to a particular locale. However, entry of virus into different regions could be inferred to occur independently as discrete events, and not from a spreading infection, leading to the segregation of regional brain clades from one another as exemplified by the phylogenetic tree of macaque 247.

A recent publication proposed viral flow between different brain regions of a single patient with HAD (Salemi *et al*, 2005); our findings suggest that in this experimental macaque infection this is not the case. The paucity of viral exchange among brain compartments in this study was apparent even in macaque 362, which demonstrated the least amount of compartmental structure, even among anatomically close areas such as the the caudate and the area surrounding the lateral ventricle. Anatomically the head of the caudate nucleus forms part of the floor of the anterior horn of the lateral ventricle, whereas the body of the caudate form the lateral wall of the lateral ventricle and the tail of the caudate borders the inferior horn of the lateral ventricle. Nevertheless, the physical continuity of the caudate and the lateral ventricle did not translate into phylogenetic proximity. Instead, the caudate sequences related to sequences from the spleen and colon, indicating that the source of the virus in the caudate was most likely a circulating virus that also entered into the spleen and colon. This pattern of unrelated regional brain clades was also seen in the phylogenetic trees of the other three macaques, where several brain regions shared a most common recent ancestor with nonbrain regions. Examples included the cerebellum and spinal cord of macaque 247, the cerebrum, cerebellum, and the lateral ventricle of macaque 190, and the lateral ventricle of macaque 264.

In this regard, Korber and colleagues demonstrated that envelopes sampled from the brain of an HIV-infected individual at a second time point were phylogenetically more related to sequences from the blood sampled at a first time point taken 6 weeks earlier than to sequences isolated from the brain at the first time point (Korber *et al*, 1994). This suggests that viruses from circulation enter into the brain at multiple times throughout infection. Although longitudinal sampling of macaque brains is not experimentally feasible for practical and ethical reasons, the use of a known clonal inoculum allows for inference of times of origin of the isolated CNS envelopes. With a known starting sequence and using the most recent common ancestor (MRCA) for a regional clade as the founding virus for its neuroanatomical locale of origin, the relative times of viral entry into different regions could be inferred from the horizontal distance of the MRCAs from the initial parental SIVmac239 on the phylogenetic trees. As exemplified in the tree of macaque 247 (Figure 1A), phylogenetic inference of the distance of regional MRCAs from SIVmac239 suggests that entry into the cerebellum and spinal cord occurred later than entry into the cerebrum and the region surrounding the third ventricle.

Interestingly, the cerebellum and spinal cord of this macaque were also the two compartments from which envelopes containing mutations in the GGGDPE motif that forms part of the CD4-binding site were isolated. We demonstrated in cell-cell fusion assays that for the cerebellar envelopes, the G383E mutation can contribute to a CD4-independent and neutralization sensitive phenotype, consistent with previous reports indicating that mutations in this region may affect CD4 utilization (Dehghani *et al*, 2003; Kodama *et al*, 1993; Ryzhova *et al*, 2002a). Although it is tempting to hypothesize that the acquisition of CD4-independence is an adaptive trait for the environment of low CD4 expression in the brain, the dn to ds test of selection did not indicate overt positive selection of these envelopes (Figure 2). An alternative hypothesis—because these envelopes were inferred to have entered later into the CNS—is that the acquisition of a CD4-independent phenotype serves as a marker for a failing immune response where neutralizing antibodies are no longer generated. Unfortunately, longitudinal blood samples from this macaque were not available to determine the presence of CD4-independent viruses or neutralizing antibodies relative to disease progression. Nonetheless, this may be a plausible hypothesis, because CD4-independent envelopes are often isolated from rapidly progressing macaques where there is a weak SIV-specific antibody response, and during the late stages of chronic infection where the immune system is failing (Bhattacharya *et al*, 2003; Dehghani *et al*, 2003; Ryzhova *et al*, 2002a; Vodros *et al*, 2003). Alternatively, CD4-independence may be an adaptive feature but not be acquired because the viral population dynamics within the CNS are not conducive for favorable traits to be fixed in the population. Such a scenario would arise in a setting where the effective size of the population is below the threshold required for deterministic evolution to occur and instead, evolution occurs by random genetic drift (Brown, 1997; Coffin, 1996; Frost *et al*, 2001). The existence of several smaller and independent populations within the brain as evidenced by regional clades in the phylogenetic trees would present a setting where the evolutionary dynamics would favor a stochastic process and hence favorable traits such as CD4-independence may not be acquired.

One important limitation of this study is the number of sequences sampled for each region. Due to the difficulty of phylogenetic computations with long sequences and large numbers of sequences, we were limited in the number of sequences sampled for each region. Because of this limitation, the sequences isolated may not have been representative of the predominant species present in the DNA and the method of polymerase chain reaction (PCR) amplification may favor amplification of certain genotypes over others. Despite this potential bias, PCR amplification

is currently used in other labs to study phylogenetic relationships and diversity of genotypes (Ohagen *et al*, 2003; Salemi *et al*, 2005). Furthermore, in this study, additional PCR amplifications for at least one brain region for each macaque resulted in similar phylogenetic relationships. These additional sequences were not included in Figure 1 for clarity of representing the phylogenetic relationships. Current work is in progress with other macaques to address whether these phylogenetic relationships are reproducible with greater sampling.

In summary, we have analyzed DNA sequences from tissues of four SIVmac239-infected rhesus macaques and examined regional differences among the *env* genes. We demonstrate that similar to HIV infection in humans, SIV also demonstrates regional CNS compartmentalization despite the use of a controlled, homogenous inoculum. The degree of compartmentalization strengthened with increased disease progression and occurred regardless of the presence or absence of pathological presence of giant-cell encephalitis. Using one discrete group of envelopes from the cerebellum of one animal as illustrated, we have also shown that there are potential region-specific phenotypes of neutralization escape and receptor utilization. These studies highlight the importance of analyzing multiple regions of an organ in studies designed to characterize viral genotypes of specific organs.

Materials and methods

Tissue collection and processing
Tissue specimens were obtained from the archived collection of rhesus macaque tissues housed at the New England Regional Primate Research Center (Southborough, MA), generous gifts of Drs. Ronald Desrosiers and Keith Mansfield. Briefly, all macaques were intravenously inoculated with the molecular-cloned virus, SIVmac239 at a dose of 50 ng p27/kg. At necropsy, brain tissues were collected and fixed in 10% neutral buffered formalin, embedded in paraffin, sectioned at 6 μM and stained with hematoxylin and eosin by routine techniques for determination of presence of inflammatory changes and giant cells in the CNS. An expert pathologist examined sufficient slides to determine the extent of the pathology for the classification of giant cell encephalitis. Adjacent blocks of fresh tissue were snap frozen in optimum cutting temperature compound (O.C.T.; Miles, Elkhart, IN) by immersion in 2-methylbutane cooled in dry ice.

Cloning and sequencing of envelope gp160
Genomic DNA was isolated from frozen tissue using the DNeasy Tissue Kit (Qiagen Inc.). Genomic DNA, 50 to 150 ng, was used in nested PCR reactions for amplification of the entire envelope gp160 using a high fidelity polymerase (rTth DNA polymerase XL; Applied Biosystems) with the following primers: outer, 239env6808 (5′-GAACTCCGAAAAAGGCTAAGGC-3′) (bases 6808 to 6829 of SIVmac239 genome) and 239env9541 (5′-CTCTCTCTTCAGCTGGGTTTCTCC-3′) (bases 9541 to 9564); and inner, SIVenvXBA (5′-GCTCTAGAAT GGGATGTCTTGGGAATCAGCTGC-3′) (bases 6860-6884, Xbal restriction site incorporated into primer is underlined), SIVenvKPN (5′-CCGGTACC TCACAAGAGAGTGAGCTCAAGCCC-3′ (bases 9476 to 9498, Kpnl restriction site incorporated into primer is underlined). PCR products were cloned into pcDNA3.1 (Invitrogen) using the Xbal and Kpnl restriction sites, clones with gp160 were selected, and nucleotide sequencing was performed at the DNA sequencing facility operated by the Department of Genetics, University of Pennsylvania.

Sequence and phylogenetic analysis
Sequences were aligned using MacVector 7.2.2. Phylogenies were constructed under parsimony and maximum likelihood criteria using PAUP* v4.0b10 (Swofford, 2002). Neighbor-joining trees were constructed using MacVector 7.2.2. For all three phylogenetic methods, SIVmac239 gp160 sequence was the out-group to which the trees are rooted. Parsimony analysis was performed by tree-bisection-reconnection (TBR) branch swapping on 100 random stepwise addition trees. Bootstrap support was established from searches on 100 pseudoreplicate data sets. For maximum likelihood analysis, the best-fit model was determined for each data set using ModelTest v3.06 (Posada, 2001). Maximum likelihood heuristic tree searches with TBR branch-swapping were conducted on 10 stepwise addition trees with random taxon addition. Bootstrap support for each clade was established from 100 replicate analysis.

Nucleotide distance analysis
Pairwise nucleotide distances, synonymous and non-synonymous substitutions and sites were calculated using the Kimura two-parameter model on MEGA3 (Kumar *et al*, 2004). For each sequence, ds and dn were determined from the pairwise distance between each envelope sequence and the starting SIVmac239 sequence. Statistics were performed by the software program XLSTAT-Pro using *t* test for ds:dn comparisons within a tissue region and the Mann-Whitney *U* test for comparisons between different tissues and for unpaired samples.

Phylogenetic compartmental structure analysis
A phylogenetic evaluation of the presence of tissue compartmentalization of SIV gp160 was performed using a modified Slatkin-Maddison test (Poss *et al*, 1998; Slatkin and Maddison, 1990). Briefly, a new *n*-state character was created for each macaque sample where n = the number of tissues sampled. For example, for macaque 247, 6 different tissue/brain regions were sampled and hence a new 6-state character

was created for macaque 247. Each sequence was assigned a state for this new character based on the tissue/brain region from which it was isolated. As an example, for macaque 247, cerebrum = 1, cerebellum = 2, periventricle = 3, spinal cord = 4, colon = 5, and MesLN = 6. The fewest number of evolutionary steps (*s*) required to fit the tissue-compartment character on the phylogenetic tree was performed using MacClade 4.06 (Maddison and Maddison, 2003). For a phylogenetic tree with complete compartmental structure, the number of evolutionary steps (*s*) is the number of compartments (*n*) minus 1. Should a sequence from a brain region/tissue sample not cluster with all of the other sequences from that region/tissue, a migration event is said to have occurred and the number of evolutionary steps required to fit the tissue-compartment character on the tree will increase an additional step. Calculation of the number of steps (*s*) was performed for 100 bootstrap trees and the average and variance of *s* were determined. The test for compartmentalization was performed on the sample distribution of bootstrap *s* compared to the null distribution of s from 100 random trees with no compartment structure generated by MacClade 4.06 using the random joining/splitting option. If there is compartmental structure, the bootstrap *s* should be significantly less than *s* from random trees. Hence the null hypothesis of no compartmental structure is rejected if the ratio of bootstrap *s* to random *s* is less than 1.

Phenetic compartmental structure analysis

Mantel's test was performed as previously described to determine if the sequences from any compartment share more genetic identity with each other than with sequences in other compartments (Mantel, 1967; Poss *et al*, 1998). Briefly, for each macaque, a distance matrix consisting of pairwise Kimura two-parameter distances of all sequences from that macaque was generated by MEGA3. A second matrix was generated such that $M(i, j) = 0$ if the sequence i is from the same compartment as sequence j, 1 if the sequence i is from a different compartment as sequence j. The test statistic is the Pearson correlation coefficient, r, computed for all pairs of the elements of both matrices, except for the diagonal. The null distribution was constructed by permuting the compartment matrix 1000 times and calculating r for each permutation. The hypothesis of compartmental structure is rejected if more than 5% of the null distribution exceeds the sample r. Calculation of the Pearson correlation coefficients, permutations of the compartment matrix, and statistical testing were performed with the *XL*STAT-Pro program.

Cell-cell fusion assay

A cell-cell fusion assay was performed as previously described (Edinger, 1999). Briefly, effector cells transiently expressing gp160 were generated by infected QT6 cells in 6-well tissue culture plates with vaccinia virus vTF1.1 (gift of B. Puffer, University of Pennsylvania) at an multiplicity of infection (MOI) of 10 for 1 h at 37°C and transfected for 4 h by standard calcium phosphate method with 3 μg/well of the desired gp160-expressing plasmid. Cells were incubated overnight with rifampin at a concentration of 100 μg/ml at 32°C. Target cells transiently expressing the desired receptors (either rhesus CD4, rhesus CCR5, or both) and a T7 luciferase reporter plasmid were generated by transfecting QT6 cells in 48-well plates in a total of 1 μg/well by calcium phosphate and allowed to express overnight. Effector cells were mixed with receptor target cells and cell-cell fusion was assessed 8 h later by adding luciferase substrate (Promega) with cell lysates and quantifying luciferase activity with a Packard LumiCount luminometer.

For neutralization studies, target cells were incubated with pooled plasma from SIV239-infected macaques at the plasma dilutions indicated for 1 h at 37°C and then added onto effector cells as described above.

Site-directed mutagenesis

Site-directed mutagenesis to revert glutamic acid (E) at amino acid position 383 back to glycine (G) of the parental SIVmac239 clone was performed using the QuikChange site-directed mutagenesis kit (Strategene). Reversion clones were sequenced to ensure that no additional changes other than the intended mutations were present.

Nucleotide sequences

Gp160 sequences used to construct phylogenetic trees were submitted to Genbank (Accession numbers DQ136192 to DQ136310).

References

Anderson MG, Hauer D, Sharma DP, Joag SV, Narayan O, Zink MC, Clements JE (1993). Analysis of envelope changes acquired by SIVmac239 during neuroadaption in rhesus macaques. *Virology* **195:** 616–626.

Babas T, Munoz D, Mankowski JL, Tarwater PM, Clements JE, Zink, MC (2003). Role of microglial cells in selective replication of simian immunodeficiency virus genotypes in the brain. *J Virol* **77:** 208–216.

Bhattacharya J, Peters PJ, and Clapham, PR (2003). CD4-independent infection of HIV and SIV: implications for envelope conformation and cell tropism in vivo. *AIDS* **17 (Suppl 4):** S35–S43.

Brown AJ (1997). Analysis of HIV-1 env gene sequences reveals evidence for a low effective number in the viral population. *Proc Natl Acad Sci USA* **94:** 1862–1865.

Campbell BJ, Hirsch VM (1994). Extensive envelope heterogeneity of simian immunodeficiency virus in tissues from infected macaques. *J Virol* **68:** 3129–3137.

Chen B, Vogan EM, Gong H, Skehel JJ, Wiley DC, Harrison SC (2005). Structure of an unliganded simian immunodeficiency virus gp120 core. *Nature* **433:** 834–841.

Clements JE, Babas T, Mankowski JL, Suryanarayana K, Piatak M, Jr Tarwater PM, Lifson JD, Zink MC (2002). The central nervous system as a reservoir for simian immunodeficiency virus (SIV): steady-state levels of SIV DMA in brain from acute through asymptomatic infection. *J Infect Dis* **186:** 905–913.

Coffin JM (1995). HIV population dynamics in vivo: implications for genetic variation, pathogenesis, and therapy. *Science* **267:** 483–489.

Coffin JM (1996). HIV viral dynamics. *AIDS* **10 (Suppl 3):** S75–S84.

Crandall KA, Kelsey CR, Imamichi H, Salzman NP (1999). Parallel evolution of drug resistance in HIV: failure of nonsynonymous/synonymous substitution rate ratio to detect selection. *Mol Biol Evol* **16:** 372–382.

Dehghani H, Puffer BA, Doms RW, Hirsch VM (2003). Unique pattern of convergent envelope evolution in simian immunodeficiency virus-infected rapid progressor macaques: association with CD4-independent usage of CCR5. *J Virol* **77:** 6405–6418.

Edinger AL, Doms RW (1999). A cell-cell fusion assay to moniter HIV-1 Env interactions with chemokine receptors. Methods in molecular medicine, Michael NL and Kim JH (eds). Totowa, NJ: Humana Press. 17: 41–49.

Fox HS, Gold LH, Henriksen SJ, Bloom FE (1997). Simian immunodeficiency virus: a model for neuroAIDS. *Neurobiol Dis* **4:** 265–274.

Frost SD, Dumaurier MJ, Wain-Hobson S, Brown AJ (2001). Genetic drift and within-host metapopulation dynamics of HIV-1 infection. *Proc Natl Acad Sci USA* **98:** 6975–6980.

Fulcher JA, Hwangbo Y, Zioni R, Nickle D, Lin X, Heath L, Mullins JI, Corey L, Zhu T (2004). Compartmentalization of human immunodeficiency virus type 1 between blood monocytes and CD4+ T cells during infection. *J Virol* **78:** 7883–7893.

Gendelman HE, Lipton SA, Tardieu M, Bukrinsky MI, Nottet HS (1994). The neuropathogenesis of HIV-1 infection. *J Leukoc Biol* **56:** 389–398.

Glass JD, Fedor H, Wesselingh SL, McArthur JC (1995). Immunocytochemical quantitation of human immunodeficiency virus in the brain: correlations with dementia. *Ann Neurol* **38:** 755–762.

Gorry PR, Bristol G, Zack JA, Ritola K, Swanstrom R, Birch CJ, Bell JE, Bannert N, Crawford K, Wang H, Schols D, De Clercq E, Kunstman K, Wolinsky SM, Gabuzda D (2001). Macrophage tropism of human immunodeficiency virus type 1 isolates from brain and lymphoid tissues predicts neurotropism independent of coreceptor specificity. *J Virol* **75:** 10073–10089.

Hirsch VM, Dapolito G, Hahn A, Lifson J, Montefiori D, Brown CR, Goeken R (1998). Viral genetic evolution in macaques infected with molecularly cloned simian immunodeficiency virus correlates with the extent of persistent viremia. *J Virol* **72:** 6482–6489.

Kimata JT, Gosink JJ, KewalRamani VN, Rudensey LM, Liftman DR, Overbaugh J (1999). Coreceptor specificity of temporal variants of simian immunodeficiency virus Mne. *J Virol* **73:** 1655–1660.

Kinsey NE, Anderson MG, Unangst TJ, Joag SV, Narayan O, Zink MC, Clements JE (1996). Antigenic variation of SIV: mutations in V4 alter the neutralization profile. *Virology* **221:** 14–21.

Kodama T, Mori K, Kawahara T, Ringler DJ, Desrosiers RC (1993). Analysis of simian immunodeficiency virus sequence variation in tissues of rhesus macaques with simian AIDS. *J Virol* **67:** 6522–6534.

Kolchinsky P, Kiprilov E, Sodroski J (2001). Increased neutralization sensitivity of CD4-independent human immunodeficiency virus variants. *J Virol* **75:** 2041–2050.

Korber BT, Kunstman KJ, Patterson BK, Furtado M, McEvilly MM, Levy R, Wolinsky SM (1994). Genetic differences between blood- and brain-derived viral sequences from human immunodeficiency virus type 1-infected patients: evidence of conserved elements in the V3 region of the envelope protein of brain-derived sequences. *J Virol* **68:** 7467–7481.

Kumar S, Tamura K, Nei M (2004). MEGA 3: integrated software for molecular evolutionary genetics analysis and sequence alignment. *Brief Bioinformat* **5:** 150–163.

Kwong PD, Wyatt R, Robinson J, Sweet RW, Sodroski J, Hendrickson WA (1998). Structure of an HIV gp120 envelope glycoprotein in complex with the CD4 receptor and a neutralizing human antibody. *Nature* **393:** 648–659.

Lackner AA, Smith MO, Munn RJ, Martfeld DJ, Gardner MB, Marx PA, Dandekar S (1991). Localization of simian immunodeficiency virus in the central nervous system of rhesus monkeys. *Am J Pathol* **139:** 609–621.

Lin G, Baribaud F, Romano J, Doms RW, Hoxie JA (2003). Identification of gp120 binding sites on CXCR4 by using CD4-independent human immunodeficiency virus type 2 Env proteins. *J Virol* **77:** 931–942.

Liu Y, Tang XP, McArthur JC, Scott J, Gartner S (2000). Analysis of human immunodeficiency virus type 1 gp160 sequences from a patient with HIV dementia: evidence for monocyte trafficking into brain. *J NeuroVirol* **6 (Suppl 1):** S70–S81.

Maddison DR, Maddison WP (2003). MacClade 4: Analysis of phylogeny and character evolution. Sunderland, MA: Sinauer Associates.

Mankowski JL, Flaherty MT, Spelman JP, Hauer DA, Didier PJ, Amedee AM, Murphey-Corb M, Kirstein LM, Munoz A, Clements JE, Zink MC (1997). Pathogenesis of simian immunodeficiency virus encephalitis: viral determinants of neurovirulence. *J Virol* **71:** 6055–6060.

Mantel N (1967). The detection of disease clustering and a generalized regression approach. *Cancer Res* **27:** 209–220.

Martin J, LaBranche CC, Gonzalez-Scarano F (2001). Differential CD4/CCR5 utilization, gp120 conformation, and neutralization sensitivity between envelopes from a microglia-adapted human immunodeficiency virus type 1 and its parental isolate. *J Virol* **75:** 3568–3580.

McArthur JC, Sacktor N, Seines, O (1999). Human immunodeficiency virus-associated dementia. *Semin Neurol* **19:** 129–150.

Ohagen A, Devitt A, Kunstman KJ, Gorry PR, Rose PP, Korber B, Taylor J, Levy R, Murphy RL, Wolinsky SM, Gabuzda D (2003). Genetic and functional analysis of full-length human immunodeficiency virus type 1 env genes derived from brain and blood of patients with AIDS. *J Virol* **77:** 12336–12345.

Overbaugh J, Rudensey LM, Papenhausen MD, Benveniste RE, Morton WR (1991). Variation in simian immunodeficiency virus env is confined to V1 and V4 during progression to simian AIDS. *J Virol* **65:** 7025–7031.

Perelson AS, Neumann AU, Markowitz M, Leonard JM, Ho DD (1996). HIV-1 dynamics in vivo: virion clearance rate, infected cell life-span, and viral generation time. *Science* **271:** 1582–1586.

Peters PJ, Bhattacharya J, Hibbitts S, Dittmar MT, Simmons G, Bell J, Simmonds P, Clapham PR (2004). Biological analysis of human immunodeficiency virus type 1 R5 envelopes amplified from brain and lymph node tissues of AIDS patients with neuropathology reveals two distinct tropism phenotypes and identifies envelopes in the brain that confer an enhanced tropism and fusigenicity for macrophages. *J Virol* **78:** 6915–6926.

Posada D (2001). ModelTest 3.06. Boston, MA: Free Software Foundation.

Poss M, Rodrigo AG, Gosink JJ, Learn GH, de Vange Panteleeff D, Martin HL, Jr, Bwayo J, Kreiss JK, Overbaugh J (1998). Evolution of envelope sequences from the genital tract and peripheral blood of women infected with clade A human immunodeficiency virus type 1. *J Virol* **72:** 8240–8251.

Power C, McArthur JC, Johnson RT, Griffin DE, Glass JD, Perryman S, Chesebro B (1994). Demented and nondemented patients with AIDS differ in brain-derived human immunodeficiency virus type 1 envelope sequences. *J Virol* **68:** 4643–4649.

Price RW, Brew B, Sidtis J, Rosenblum M, Scheck AC, Cleary P (1988). The brain in AIDS: central nervous system HIV-1 infection and AIDS dementia complex. *Science* **239:** 586–592.

Prospero-Garcia O, Gold LH, Fox HS, Polls I, Koob GF, Bloom FE, Henriksen SJ (1996). Microglia-passaged simian immunodeficiency virus induces neurophysiological abnormalities in monkeys. *Proc Natl Acad Sci USA* **93:** 14158–14163.

Puffer BA, Altamura LA, Pierson TC, Doms RW (2004). Determinants within gp120 and gp41 contribute to CD4 independence of SIV Envs. *Virology* **327:** 16–25.

Puffer BA, Pohlmann S, Edinger AL, Carlin D, Sanchez MD, Reitter J, Watry DD, Fox HS, Desrosiers RC, Doms RW (2002). CD4 independence of simian immunodeficiency virus Envs is associated with macrophage tropism, neutralization sensitivity and attenuated pathogenicity. *J Virol* **76:** 2595–2605.

Ryzhova E, Whitbeck JC, Canziani G, Westmoreland SV, Cohen GH, Eisenberg RJ, Lackner A, Gonzalez-Scarano F (2002a). Rapid progression to simian AIDS can be accompanied by selection of CD4-independent gp120 variants with impaired ability to bind CD4. *J Virol* **76:** 7903–7909.

Ryzhova EV, Crino P, Shawver L, Westmoreland SV, Lackner, AA, Gonzalez-Scarano F (2002b). Simian immunodeficiency virus encephalitis: analysis of envelope sequences from individual brain multinucleated giant cells and tissue samples. *Virology* **297:** 57–67.

Sacktor N, Lyles RH, Skolasky R, Kleeberger C, Seines OA, Miller EN, Becker JT, Cohen B, McArthur JC. (2001a). HIV-associated neurologic disease incidence changes: Multicenter AIDS Cohort Study, 1990–1998. *Neurology* **56:** 257–260.

Sacktor N, McDermott MP, Marder K, Schifitto G, Seines OA, McArthur JC, Stern Y, Albert S, Palumbo D, Kieburtz K, De Marcaida JA, Cohen B, Epstein, L (2002). HIV-associated cognitive impairment before and after the advent of combination therapy. *J NeuroVirol* **8:** 136–142.

Sacktor N, Tarwater PM, Skolasky RL, McArthur JC, Seines OA, Becker J, Cohen B, Miller EN (2001 b). CSF antiretroviral drug penetrance and the treatment of HIV-associated psychomotor slowing. *Neurology* **57:** 542–544.

Salemi M, Lamers SL, Yu S, de Oliveira T, Fitch WM, McGrath MS (2005). Phylodynamic analysis of human immunodeficiency virus type 1 in distinct brain compartments provides a model for the neuropathogenesis of AIDS. *J Virol* **79**: 11343–11352.

Shapshak P, Segal DM, Crandall KA, Fujimura RK, Zhang BT, Xin KQ, Okuda K, Petito CK, Eisdorfer C, Goodkin K (1999). Independent evolution of HIV type 1 in different brain regions. *AIDS Res Hum Retroviruses* **15:** 811–820.

Sharp PM (1997). In search of molecular darwinism. *Nature* **385:** 111–112.

Shriner D, Shankarappa R, Jensen MA, Nickle DC, Mittler JE, Margolick JB, Mullins JI (2004). Influence of random genetic drift on human immunodeficiency virus type 1 env evolution during chronic infection. *Genetics* **166:** 1155–1164.

Slatkin M, Maddison WP (1990). Detecting isolation by distance using phylogenies of genes. *Genetics* **126:** 249–260.

Smit TK, Brew BJ, Tourtellotte W, Morgello S, Gelman BB, Saksena NK (2004). Independent evolution of human immunodeficiency virus (HIV) drug resistance mutations in diverse areas of the brain in HIV-infected patients, with and without dementia, on antiretroviral treatment. *J Virol* **78:** 10133–10148.

Smit TK, Wang B, Ng T, Osborne R, Brew B, Saksena NK (2001). Varied tropism of HIV-1 isolates derived from different regions of adult brain cortex discriminate between patients with and without AIDS dementia complex (ADC): evidence for neurotropic HIV variants. *Virology* **279:** 509–526.

Swofford D (2002). PAUP*: phylogenetic analysis using parsimony (*and other methods) 4.0b10. Sunderland, MA: Sinauer Associates.

Vazeux R, Lacroix-Ciaudo C, Blanche S, Cumont MC, Henin D, Gray F, Boccon-Gibod L, Tardieu M (1992). Low levels of human immunodeficiency virus replication in the brain tissue of children with severe acquired immunodeficiency syndrome encephalopathy. *Am J Pathol* **140:** 137–144.

Vodros D, Thorstensson R, Doms RW, Fenyo EM, Reeves JD (2003). Evolution of coreceptor use and CD4-independence in envelope clones derived from SIVsm-infected macaques. *Virology* **316:** 17–28.

Wang J, Crawford K, Yuan M, Wang H, Gorry PR, Gabuzda D (2002). Regulation of CC chemokine receptor 5 and CD4 expression and human immunodeficiency virus type 1 replication in human macrophages and microglia by T helper type 2 cytokines. *J Infect Dis* **185:** 885–897.

Wang TH, Donaldson YK, Brettle RP, Bell JE, Simmonds P (2001). Identification of shared populations of human immunodeficiency virus type 1 infecting microglia and tissue macrophages outside the central nervous system. *J Virol* **75:** 11686–11699.

Wolinsky SM, Korber BT, Neumann AU, Daniels M, Kunstman KJ, Whetsell AJ, Furtado MR, Cao Y, Ho DD, Safrit JT (1996). Adaptive evolution of human immunodeficiency virus-type 1 during the natural course of infection. *Science* **272:** 537–542.

Zhang L, Rowe L, He T, Chung C, Yu J, Yu W, Talal A, Markowitz M, Ho DD (2002). Compartmentalization of surface envelope glycoprotein of human immunodeficiency virus type 1 during acute and chronic infection. *J Virol* **76:** 9465–9473.

Zink MC, Amedee AM, Mankowski JL, Craig L, Didier P, Carter DL, Munoz A, Murphey-Corb M, Clements JE (1997). Pathogenesis of SIV encephalitis. Selection and replication of neurovirulent SIV. *Am J Pathol* **151:** 793–803.